Main-Chain Second-Order Nonlinear Optical Polymers: Random Incorporation of Amino–Sulfone Chromophores

Chengzeng Xu, Bo Wu, Mark W. Becker, and Larry R. Dalton*

Department of Chemistry, University of Southern California, Los Angeles, California 90089-1062

Peter M. Ranon, Yongqiang Shi, and William H. Steier

Department of Electrical Engineering, University of Southern California, Los Angeles, California 90089-0483

Received April 1, 1993. Revised Manuscript Received July 9, 1993®

Several nonlinear optical (NLO) polymers with amino–sulfone azobenzene chromophores randomly incorporated into the polymer backbone have been synthesized by condensation polymerization techniques. The length and content of the flexible segments are varied to study their effects on second-harmonic generation coefficients. For comparison, a side-chain polymer having virtually the same chromophore incorporated as a pendant has also been prepared. The effects of polymer structure on electric field poling efficiency and the stability of the poling-induced dipole alignment were studied. The results show that these main-chain, second-order NLO polymers, with random incorporation of the dipolar chromophores, can be efficiently poled, yielding $\chi^{(2)}$ as high as 300 pm/V. The temporal stability of the poling-induced macroscopic order is determined by the flexibility of the polymer chains and can be greatly enhanced by cross-linking the polymer backbone.

Introduction

In recent years, organic photonic materials have emerged as one of the frontiers of science and technology. Polymeric second-order nonlinear optical (NLO) materials are particularly promising for applications in photonic devices, such as electrooptic modulators and frequency doublers, due to their large optical nonlinearities, high laser damage thresholds, low dielectric constants, and excellent processibilities.[1] To meet the requirements for photonic applications, two important issues must be addressed. First, the materials must have large, nonresonant second-order optical nonlinearities. Second, the materials must have excellent temporal and thermal NLO stability.

In addressing the first issue, several approaches have been used in synthesizing NLO polymer materials. These include doping NLO dyes into amorphous polymer matrices,[2,3] attaching NLO moieties covalently onto polymer backbone as pendants,[4,5] incorporating NLO chromophores as part of a polymer mainchain,[6–13] and utilization of sequential synthesis methods.[14,15] Among these approaches, main-chain NLO polymers that have NLO chromophores as part of the backbone have received relatively little attention. Main-chain polymers can be divided into three groups with respect to the chromophore dipole arrangements along the polymer mainchains, namely, head-to-tail, head-to-head, and random. If the backbone of a main-chain NLO polymer is viewed in the extended configuration (Figure 1a–c), the chromophore dipole moments appear to add up for the head-to-tail configuration and cancel out for the head-to-head and random configurations. Because of this, only the head-to-tail configuration[6–9] (Figure 1a) has been considered for the main-chain second-order NLO polymers until very recently.[10–13] Consequently, very few main-chain NLO polymers have been prepared, compared to the large number of side-chain polymers synthesized, due to the limitations on structure design and the difficulty in synthesis of the head-to-tail polymers.

Robello, Williams, and co-workers have developed a new class of dipolar chromophores with sulfonyl groups as electron acceptors.[9,16] The sulfonyl acceptor is interesting not only for its relatively high electron accepting strength but also for the ease of introducing functional groups at its end. Indeed, Robello and co-workers have synthesized several amino–sulfone chromophores having one hydroxyl

• Abstract published in *Advance ACS Abstracts*, September 1, 1993.

(1) Prasad, P. N.; Williams, D. J. *Introduction to Nonlinear Optical Effects in Molecules and Polymers*; John Wiley & Sons: New York, 1991.
(2) Singer, K. D.; Sohn, J. E.; Lalama, S. J. *Appl. Phys. Lett.* **1986**, *49*, 248.
(3) Mortazavi, M. A.; Knoesen, A.; Kowel, S. T.; Higgins, B. G.; Dienes, A. *J. Opt. Soc. Am. B* **1989**, *6*, 733.
(4) Ye, C.; Marks, T. J.; Yang, J.; Wong, G. K. *Macromolecules* **1987**, *20*, 2322.
(5) Singer, K. D.; Kuzyk, M. G.; Holland, W. R.; Sohn, J. E.; Lalama, S. J.; Comizzoli, R. B.; Katz, H. E.; Schilling, M. L. *Appl. Phys. Lett.* **1988**, *53*, 1800.
(6) Green, G. D.; Weinschenk, III, j. I.; Mulvaney, J. E.; Hall, Jr., H. K. *Macromolecules* **1987**, *22*, 722.
(7) Stenger-Smith, J. D.; Fischer, J. W.; Henry, R. A.; Hoover, J. M.; Lindsay, G. A.; Hayden, L. M. *Makromol. Chem. Rapid Commun.* **1990**, *11*, 141.
(8) Fuso, F.; Padias, A. B.; Hall, Jr., H. K. *Macromolecules* **1991**, *24*, 1710.
(9) Köhler, W.; Robello, D. R.; Willand, C. S.; Williams, D. J. *Macromolecules* **1991**, *24*, 4589.
(10) Lindsay, G. A.; Stenger-Smith, J. D.; Henry, R. A.; Hoover, J. M.; Nissan, R. A.; Wynne, K. J. *Macromolecules* **1992**, *25*, 6075.
(11) Wright, M. E.; Mulick, S. *Macromolecules* **1992**, *25*, 6045.
(12) Xu, C.; Wu, B.; Dalton, L. R.; Ranon, P. M.; Shi, Y.; Steier, W. H. *Macromolecules* **1992**, *25*, 6716.
(13) Ranon, P. M.; Shi, Y.; Steier, W. H.; Xu, C.; Wu, B.; Dalton, L. R. *Appl. Phys. Lett.* **1993**, *62*, 2605.
(14) Li, D.; Ratner, M. A.; Marks, T. J.; Zhang, C.; Yang, J.; Wong, G. K. *J. Am. Chem. Soc.* **1990**, *112*, 7389.
(15) Katz, H. E.; Scheller, G.; Putvinski, T. M.; Schilling, M. L.; Wilson, W. L.; Chidsey, C. E. D. *Science* **1991**, *254*, 1486.
(16) Ulman, A.; Willand, C. S.; Köhler, W.; Robello, D. R.; Williams, D. J.; Handley, L. *J. Am. Chem. Soc.* **1990**, *112*, 7083.

0897-4756/93/2805-1439$04.00/0

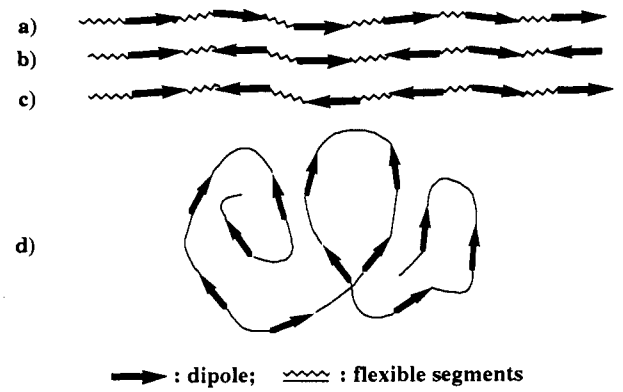

Figure 1. Chromophore dipole arrangements along the polymer mainchain: (a) head-to-tail, (b) head-to-head, (c) random, and (d) poling-induced dipole alignment in a random polymer chain.

group at one end and one ester group at the other. From these functionalized chromophores several head-to-tail main-chain NLO polymers have been synthesized.[9] In this paper, we describe the synthesis of several main-chain, second-order NLO polymers with random incorporation of the dipolar amino–sulfone chromophores. We also demonstrate that these random polymers can be efficiently poled, yielding large SHG coefficients comparable to that of the side-chain polymers containing the same chromophores.

Regarding the second issue, a primary disadvantage of poled polymer materials, as compared to crystals, is the relaxation of electric field poling-induced noncentrosymmetric order in the absence of an electric field. This order is necessary for second-order optical nonlinearity. The interaction forces among the macromolecules (van der Waals, hydrogen bonding, etc.) are not strong enough to prevent the segmental motions and pendant rotations, especially in the case of dipole-oriented states. Polymer segmental motions and pendant rotations lead to the relaxation of the ordered lattice to a thermodynamically more stable random structure. Cross-linking reactions have been employed (and proven effective) in restraining the segmental motions and facilitating stabilization of the poling-induced order.[17-27] We have recently developed a novel class of double-end cross-linkable (DEC) chromophores.[22,28] These cross-linked DEC polymer films exhibit long-term temporal NLO stability even at 125 °C. The excellent stability can be attributed to high cross-linking density and locking-in of the ends of the chromophores. These results inspired us to pursue cross-linkable main-chain, second-order NLO polymers, which we expected to afford high cross-linking density and complete locking-in of both ends of the chromophore dipoles. In this paper, we demonstrate the feasibility of achieving high stability of poling-induced order by cross-linking the polymer backbone of main-chain NLO polymers.

Experimental Section

General Methods. ^1H and ^{13}C NMR spectra were taken using a Bruker-250 spectrometer operating at 250 MHz, with tetramethylsilane (TMS) internal standard as a reference for chemical shifts. FTIR spectra were obtained using a Perkin-Elmer 1760 FTIR spectrophotometer. Melting points (mp) and glass transition temperatures (T_g) were determined by the Perkin-Elmer DSC-7 system, and thermal decomposition temperatures (T_d) were measured using the TGA-7 system, each with a heating rate of 20 °C/min under an argon atmosphere. Elemental analyses were performed by Atlantic Microlab, Inc. Polymer molecular weights were measured by size exclusion chromatography (SEC) using tetrahydrofuran (THF) as the eluent and polystyrene as the standard.

Materials. General. 4-Aminophenyl 6-hydroxyhexyl sulfone was synthesized according to the published literature procedures.[9] Dioxane and pyridine were dried by distillation over sodium and barium oxide, respectively, and stored in a drybox before use. The comonomers, methyl methacrylate, 1,6-diisocyanatohexane, and terephthaloyl chloride were purchased from Aldrich and were further purified by either vacuum distillation or recrystallization. Polymer 5 was prepared in our laboratory and its synthesis will be described elsewhere.[28] 4,4′-Diisocyanato-3,3′-dimethoxydiphenyl and *N*-(2-hydroxyethyl)-*N*-methylaniline were purchased from Pfaltz & Bauer and purified by vacuum subliming and vacuum distillation, respectively. Other materials were purchased from various chemical companies and used without further purification unless otherwise indicated.

4-Aminophenyl 2-Hydroxyethyl Sulfide. Sodium metal (2.4 g, 0.1 mol) was dissolved in 50 mL of absolute ethanol with stirring under nitrogen. 4-Aminothiophenol (12.5 g, 0.1 mol) was added in small portions, followed by the addition of 2-chloroethanol (8.0 g, 0.1 mol). The resulting mixture was heated to reflux for 1 h and filtered, and the filtrate was concentrated. The residue was dissolved in dichloromethane, and the solution was washed with water, then with a 5% $NaHCO_3$ solution, and again with water. The organic layer was dried over Na_2SO_4, and the solvent was evaporated to yield 12.8 g (76%) of slightly yellow oil. ^1H NMR (DMSO-d_6) δ 2.74 (t, J = 6.8, 2H), 3.44 (m, 2H), 4.77 (br, 1H), 5.24 (s, 2H), 6.52 (d, J = 6.4, 2H), 7.10 (d, J = 6.5, 2H).

4-Acetamidophenyl 2-Acetoxyethyl Sulfide. A solution consisting of 12.7 g (75 mmol) of 4-aminophenyl 2-hydroxyethyl sulfide, 15 g (150 mmol) of acetic anhydride, and 12 g (150 mmol) of pyridine was stirred at reflux for 2 h. The solution was poured into ice water, and the resulting mixture was extracted with ethyl acetate. The organic portion was washed with water, then with a 5% HCl solution, and again with water. The washed organic layer was dried over Na_2SO_4, and then the solvent was evacuated. The residue was dried in vacuum at 50 °C for 24 h to yield 11.9 g (63%) of a slightly brown solid. ^1H NMR ($CDCl_3$) δ 2.03 (s, 3H), 2.18 (s, 3H), 3.08 (t, J = 6.9, 2H), 4.20 (t, J = 6.9, 2H), 7.39 (d, J = 8.7, 2H), 7.44 (d, J = 8.7, 2H).

4-Aminophenyl 2-Hydroxyethyl Sulfone. 4-Acetamidophenyl 2-hydroxyethyl sulfide (11.8 g, 47 mmol) was dissolved in 55 mL of glacial acetic acid. Hydrogen peroxide (12.4 g, 30% solution) was added in small portions, and the resulting mixture was stirred at reflux for 3 h. The reaction mixture was concentrated, and the residue was dissolved in dichloromethane. The solution was washed with water and dried over $MgSO_4$, and the solvent was evaporated to obtain a tan oil. The oil was refluxed with stirring for 4 h in a solution of 35 mL of ethanol and 35 mL of concentrated hydrochloric acid. The reaction solution was neutralized with 10% NaOH, concentrated, and then extracted

(17) Eich, M.; Reck, B.; Yoon, D. Y.; Wilson, C. G.; Bjorklund, G. C. *J. Appl. Phys.* **1989**, *66*, 3241.
(18) Park, J.; Marks, T. J.; Yang, J.; Wong, G. K. *Chem. Mater.* **1990**, *2*, 229.
(19) Mandal, B. K.; Chen, Y. M.; Lee, J. Y.; Kumar, J.; Tripathy, S. K. *Appl. Phys. Lett.* **1991**, *58*, 2459.
(20) Yu, L. P.; Chan, W.; Dikshit, S.; Bao, Z.; Shi, Y.; Steier, W. H. *Appl. Phys. Lett.* **1992**, *60*, 1655.
(21) Shi, Y.; Steier, W. H.; Chen, M.; Yu, L. P.; Dalton, L. R. *Appl. Phys. Lett.* **1992**, *60*, 2577.
(22) Xu, C.; Wu, B.; Dalton, L. R.; Shi, Y.; Ranon, P. M.; Steier, W. H. *Macromolecules* **1992**, *25*, 6714.
(23) Jungbauer, D.; Reck, B.; Tweig, R.; Yoon, D. Y.; Willson, C. G.; Swalen, J. D. *Appl. Phys. Lett.* **1990**, *56*, 2610.
(24) Chen, M.; Yu, L. P.; Dalton, L. R.; Shi, Y.; Steier, W. H. *Macromolecules* **1991**, *24*, 5421.
(25) Hubbard, M. A.; Marks, T. J.; Yang, J.; Wong, G. K. *Chem. Mater.* **1989**, *1*, 167.
(26) Jeng, R. J.; Chen, Y. M.; Jain, A. K.; Kumar, J.; Tripathy, S. K. *Chem. Mater.* **1992**, *4*, 972.
(27) Jeng, R. J.; Chen, Y. M.; Jain, A. K.; Kumar, J.; Tripathy, S. K. *Chem. Mater.* **1992**, *4*, 1141.
(28) Xu, C.; Wu, B.; Dalton, L. R.; Shi, Y.; Ranon, P. M.; Steier, W. H. *Macromolecules*, in press.

with THF. The organic layer was concentrated and then purified by column chromatography using chloroform and methanol mixed solvent as an eluant to yield 2.05 g (36%) of yellow solid. ^{1}H NMR (DMSO-d_6) δ 3.24 (t, J = 6.8, 2H), 3.60 (m, 2H), 4.82 (t, J = 5.7, 1H), 6.13 (s, 2H), 6.63 (d, J = 8.2, 2H), 7.46 (d, J = 8.2, 2H). Anal. Calcd for $C_8H_{11}NO_3S$: C, 47.75; H, 5.51; N, 6.96; S, 15.93. Found: C, 47.76; H, 5.53; N, 6.90; S, 16.04.

Monomer 1. To a stirred, ice-cooled solution of 4-aminophenyl 6-hydroxyethyl sulfone (3.0 g, 11.7 mmol) in 20 mL of 6 M H_2SO_4 was added dropwise 0.9 g (13.0 mmol) of sodium nitrite in 8 mL of water. The reaction temperature was maintained below 5 °C to prevent thermal decomposition of the diazonium salt. KI starch paper was used to monitor the reaction, and the addition of sodium nitrite was stopped after the paper turned blue. After another 15 min of stirring, *N*-(2-hydroxyethyl)-*N*-methylaniline (1.76 g, 11.7 mmol) was added. The red solution formed was stirred for an additional 15 min, and 10% NaOH aqueous solution was added to adjust the pH to 6. The resulting suspension was stirred for 30 min and the precipitated product was filtered, washed with water, and dried. The product was further purified by recrystallization from dichloromethane, yielding 3.1 g of dark red powder (yield, 65%; mp, 95 °C). ^{1}H NMR ($CDCl_3$) δ 7.98 (m, 6H), 6.87 (d, J = 9.2 Hz, 2H), 3.92 (t, J = 5.5 Hz, 2H), 3.69 (t, J = 5.5 Hz, 2H), 3.61 (t, J = 6.4 Hz, 2H), 3.21 (s, 3H), 3.11 (t, J = 5.2 Hz, 2H), 1.81–1.32 (m, br, 8H). ^{13}C NMR (DMSO-d_6) δ 21.9, 24.5, 26.8, 31.7, 38.6, 53.6, 54.1, 57.8, 60.0, 111.1, 121.8, 125.3, 128.6, 138.0, 142.0, 152.2, 155.0. Anal. Calcd for $C_{21}H_{29}N_3O_4S$: C, 60.14; H, 6.92; N, 10.02; S, 7.64. Found: C, 59.91; H, 6.95; N, 9.91; S, 7.72.

Monomer 2. Monomer 2 was synthesized from 4-aminophenyl 2-hydroxyethyl sulfone using a similar procedure to that for the preparation of monomer 1. After recrystallization from methanol, a dark red powder product (yield, 70%; mp, 135 °C) was obtained. ^{1}H NMR (DMSO-d_6) δ 8.00 (d, J = 8.6 Hz, 2H), 7.91 (d, J = 8.7 Hz, 2H), 7.81 (d, J = 9.1 Hz, 2H), 6.86 (d, J = 9.2 Hz, 2H), 4.89 (vb, –OH), 3.70 (t, J = 6.4 Hz, 2H), 3.57 (m, 4H), 3.49 (t, J = 6.5 Hz, 2H), 3.32 (vb, –OH), 3.09 (s, 3H). ^{13}C NMR (DMSO-d_6) δ 155.4, 152.7, 142.5, 139.4, 129.1, 125.7, 122.1, 111.5, 58.2, 57.7, 55.1, 54.1, 39.1. Anal. Calcd for $C_{17}H_{21}N_3O_4S$: C, 56.20; H, 5.79; N, 11.57; S, 8.82. Found: C, 56.04; H, 5.78; N, 11.46; S, 8.90.

***p*-Phenylenediacrylic Acid.** This compound was synthesized using the literature procedure with modified purification procedure.[29] The pure white product (91%) was obtained by recrystallization from acetic acid, followed by washing with acetone and chloroform. ^{1}H NMR (DMSO-d_6) δ 7.71 (s, 4H), 7.59 (d, J = 16 Hz, 2H), 6.59 (d, J = 16 Hz, 2H). Anal. Calcd for $C_{12}H_{10}O_4$: C, 66.06; H, 4.60. Found: C, 66.21; H, 4.48.

***p*-Phenylenediacryloyl Chloride.** *p*-Phenylenediacrylic acid (5.0 g) was refluxed with 20 mL of thionyl chloride and 5 mL of benzene for 5 h under argon atmosphere. The resulting clear yellow solution was cooled to room temperature to yield yellow crystals, which were subsequently dried by vacuum pumping. The yellow crystals were recrystallized from benzene to afford 5.2 g (90%) of pure product. ^{1}H NMR ($CDCl_3$) δ 7.83 (d, J = 15.6 Hz, 2H), 7.65 (s, 4H), 6.72 (d, J = 15.6 Hz, 2H).

Polymer 1. Polymer 1 was synthesized by refluxing 15 mL of dioxane solution of monomer 1 (1.51 g, 3.6 mmol) and 1,6-diisocyanatohexane (0.61 g, 3.6 mmol) for 3 h under argon atmosphere. The orange polymer solid was obtained by pouring the reaction solution into excess methanol. Then it was further purified by dissolving in dioxane and precipitating in methanol again, affording 0.9 g (42%) of orange powder. ^{1}H NMR ($CDCl_3$) δ 7.94 (broad, 6H), 6.81 (d, J = 8.9 Hz, 2H), 4.70 (vb, –CON*H*–), 4.26 (t, br, 2H), 3.98 (t, br, 2H), 3.70 (br, 2H), 3.18–2.94 (m, br, 9H), 1.71–1.23 (m, br, 16H). Anal. Calcd for $C_{29}H_{41}N_5O_6S$ (repeating unit): C, 59.28; H, 6.98; N, 11.93; S, 5.45. Found: C, 58.43; H, 7.08; N, 11.63; S, 5.39.

Polymer 2. Terephthaloyl chloride (0.70 g, 1.67 mmol) in 5 mL of dioxane was added dropwise into 15 mL of stirred dioxane solution containing monomer 1 (0.346 g, 1.70 mmol) and pyridine (0.5 mL). The reaction solution was refluxed for 14 h, cooled to room temperature, and precipitated in methanol. The polymer precipitate was collected by filtration and then purified by reprecipitating in methanol, yielding 0.33 g (36%) of orange powder. ^{1}H NMR ($CDCl_3$) δ 7.93 (m, br, 10H), 6.86 (br, 2H), 4.57 (t, J = 4.3 Hz, 2H), 4.30 (br, 2H), 3.89 (br, 2H), 3.15 (br, 5H), 1.74 (br, 4H), 1.43 (br, 4H).

Table I. Poling Conditions for the NLO Polymers

film (polymer)	thickness (μm)	temp (°C)	time (min)	voltage (kV)
1	0.33	125	30	6
1[a]	1.20	125	120	6
2	0.30	110	45	5
3	0.25	120	30	6
4	0.17	110–115	45	5
5	1.13	125	45	10

[a] Polymer 1 containing the cross-linker dianisidine diisocyanate.

Polymer 3. This polymer was synthesized using a similar procedure to that for polymer 2. Thus, monomer 2 (0.85 g, 2.33 mmol), terephthaloyl chloride (0.49 g, 2.42 mmol), and pyridine (0.3 mL), in 20 mL of dioxane were refluxed for 14 h under argon. After precipitating in methanol, 0.26 g (24%) of orange powder was obtained. ^{1}H NMR ($CDCl_3$) δ 8.07–7.61 (m, vb, 10H), 6.83 (br, 2H), 4.72 (br, 2H), 4.58 (br, 2H), 3.78–3.66 (vb, 4H), 3.13 (br, 3H).

Polymer 4. Dioxane solution of monomer 1 (0.304 g, 1.20 mmol), phenylenediacryloyl chloride (0.50 g, 1.20 mmol) and pyridine (0.5 mL) were refluxed for 14 h under argon. The resulting solution was cooled and poured into methanol. The precipitate was collected by filtration, reprecipitaed in methanol and vacuum dried, yielding 0.28 g (64%) of orange solid. ^{1}H NMR ($CDCl_3$) δ 8.00 (br, 6H), 7.47 (vb, 6H), 7.20 (br, 2H), 6.96 (d, br, 2H), 6.46 (br, 2H), 4.48 (br, 2H), 4.19 (br, 2H), 3.88 (br, 2H), 3.16 (br, 5H), 1.68–1.43 (vb, 8H).

NLO Samples. The polymers are all soluble in common organic solvents. Optical quality thin films of polymers 1–5 were fabricated by spin casting onto indium–tin oxide (ITO) coated glass slides from 2–10% solutions in chloroform. To prepare the cross-linked film, a 10% chloroform solution containing polymer 1 and the cross-linker (4,4′-diisocyanato-3,3′-dimethoxydiphenyl), at a 1:1 molar ratio, was filtered through a 0.2-μm syringe filter and spin cast onto an ITO glass substrate. The films then subsequently dried in vacuum and poled at elevated temperatures using an ITO-grounded corona-discharge setup, with a tip-to-plane distance of 1.5–2.0 cm. The poled polymer films were then cooled to room temperature in the presence of the electric field. The poled films were measured to be 0.3–1.5 μm thick with a Dektak IIA profiler. The poling voltage and temperature, which affect the poling efficiency, were so selected that the poling efficiency was optimized while the film quality was preserved. The poling conditions for various polymer samples are listed in Table I.

Optical Measurement. The absorption spectra of the polymer films, before and after electric field poling, were measured with a Cary 2415 spectrophotometer operating in the range 300–2500 nm.

Second-harmonic generation (SHG) was employed to study the NLO properties of the polymer films. A Spectro-Physics DCR-11 mode-locked, Q-switched Nd:YAG laser (λ = 1.064 μm) with pulse width of <10 ns and repetition rate of 10 Hz was used as the fundamental source. A Y-cut quartz crystal (d^r_{11} = 0.5 pm/V) was used as the reference. The quartz crystal was at ca. 6° angle to the incident laser beam and the sample film was at a 45° angle to the incident beam.

The effective SHG coefficient of a NLO polymer, d^p_{eff}, can be calculated from the comparison of the second harmonic signals between the reference and the sample using the following equation:

$$d^p_{eff} = d^r_{11} \times \sqrt{\frac{I_p}{I_r}} \frac{n_{2\omega,p} L_{c,r} \sqrt{T_{2,\omega,r}}\, t_{\omega,r}{}^2}{n_{2\omega,r} L_{c,p} \sqrt{T_{2\omega,p}}\, t_{\omega,p}{}^2} \frac{e^{\alpha L/4} \sqrt{1 + (\alpha L/2\pi)^2 (L_{c,p}/L)^2}}{\sqrt{\sinh^2(\alpha L/4) + \sin^2(\pi L/2L_{c,p})}} \quad (1)$$

where I is the SHG intensity, $n_{2\omega}$ is the refractive index at the

(29) Ruggli, P.; Theilheimer, W. *Helv. Chim. Acta* 1941, *24*, 899.

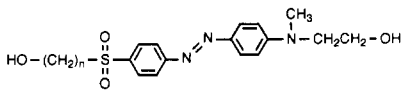

Monomer 1, n = 6; Monomer 2, n = 2

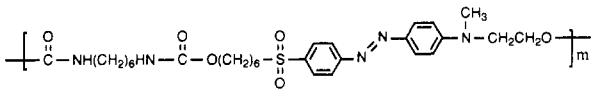

Polymer 1

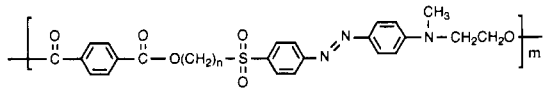

Polymer 2, n = 6; Polymer 3, n = 2

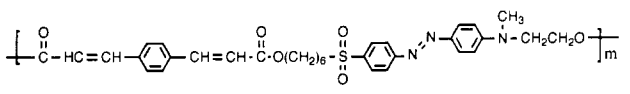

Polymer 4

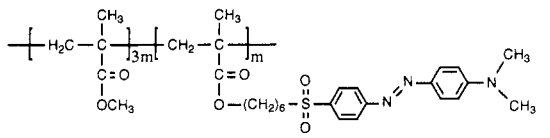

Polymer 5

Figure 2. Chemical structures of the monomers and polymers.

second harmonic (SH) wavelength, L_c is the coherence length, $T_{2\omega}$ is the transmittance at the SH wavelength, t_ω is the amplitude transmission coefficient at the fundamental wavelength, α is the absorption coefficient of the polymer film at 2ω ($\approx 2\ \mu m^{-1}$), L is the thickness of the polymer film, and the subscripts p and r denote polymer sample and reference, respectively. The refractive indexes were measured with an ellipsometer at three wavelengths using the four-zone averaging method. The coherence length (L_c) can be calculated from the refractive indexes (n_ω and $n_{2\omega}$) and the transmitted angles (θ_ω and $\theta_{2\omega}$) by the equation

$$L_c = \lambda/4(n_{2\omega}\cos\theta_{2\omega} - n_\omega\cos\theta_\omega) \quad (2)$$

For the p-polarized incident fundamental beam that we used in our measurement, d_{33} of the polymer sample can be obtained, after geometry correction, by the equation

$$d_{eff}^{p} = \left[\left({}^1/_3\cos^2\theta_\omega + \sin^2\theta_\omega\right)\sin\theta_{2\omega} + {}^2/_3\cos\theta_\omega\sin\theta_\omega\cos\theta_{2\omega}\right]d_{33} \quad (3)$$

Results and Discussion

Synthesis and Characterization of Materials. 4-Aminophenyl 6-hydroxyhexyl sulfone was synthesized using the modified literature methods.[9] 4-Aminophenyl 2-hydroxyethyl sulfone was synthesized according to the same reaction scheme at a relatively low yield. The low yield was primarily caused by the high solubility of the compound in water. Monomers 1 and 2 were synthesized using the standard diazonium coupling reactions. After recrystallization, these monomers gave satisfactory NMR and elemental analysis results, as listed in the Experimental Section.

The main-chain NLO polymers were synthesized by well-developed condensation polymerization methods. The structures of the polymers are shown in Figure 2. Polymer 1 is a polyurethane, polymers 2–4 are polyesters, and polymer 5 is an acrylate polymer. The formation of the polymers was demonstrated by NMR, FTIR, and size exclusion chromatography (SEC). Table II lists the characteristic NMR and FTIR peaks of the polymers. The new proton chemical shifts associated with the urethane or ester linkages together with the disappearance of the chemical shifts of $-CH_2OH$ in the monomers clearly indicate the formation of the polymers. The strong FTIR carbonyl bands ($\approx$1700 cm^{-1}) of the urethane or ester linkages also demonstrate the formation of the polymers. In addition, the retention of other characteristic NMR chemical shifts and FTIR bands from the chromophore monomers and comonomers prove the incorporation of the monomers into the polymers.

Table II. Characteristic NMR and FTIR Peaks of the Polymers[a]

materials	linking points (structure)	^{1}H NMR (ppm) (underlined)	FTIR (cm^{-1}) (carbonyl)
monomer 1	HOC<u>H</u>$_2$(CH$_2$)$_4$–Ch–C<u>H</u>$_2$OH	3.92, 3.61	
monomer 2	HOC<u>H</u>$_2$–Ch–C<u>H</u>$_2$OH	3.70, 3.60	
polymer 1	–Ch*–CH$_2$O<u>CO</u>N<u>H</u>CH$_2$–	4.22, 4.66, 3.14	1697
polymer 1	–Ch–(CH$_2$)$_4$CH$_2$O<u>CO</u>N<u>H</u>CH$_2$–	3.94, 4.66, 3.14	1697
polymer 2	–<u>CO</u>OCH$_2$(CH$_2$)$_4$–Ch–CH$_2$O–	4.57, 4.30	1718
polymer 3	–<u>CO</u>OCH$_2$–Ch–CH$_2$O–	4.72, 4.48	1723
polymer 4	–<u>CO</u>OCH$_2$(CH$_2$)$_4$–Ch–CH$_2$O–	4.47, 4.18	1709

[a] Ch is the chromophore unit:

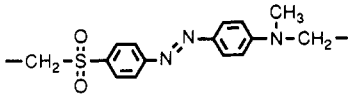

Table III. Some Physical Properties of the Polymers

polymer	$\bar{M}_w$	$\bar{M}_n$	NLO wt %	T_g (°C)	T_d (°C)
1	8000	5000	52	62	275
2	7000	4000	55	114	280
3	6800	4100	62	132	240
4	8500	4600	53	108	298
5	178000	44000	36	124	245

A summary of some properties of the polymers is given in Table III. The weight average molecular weights of the main-chain polymers measured by SEC are typically 8000 with polydispersities around 2. The NLO chromophore weight fraction in the polymers (NLO wt %) was calculated using the most basic donor–bridge–acceptor structure (see Ch structure in the footnote of Table II) as the effective unit. As can be seen from Table III, a high chromophore loading density can be realized in the main-chain polymers. The glass transition temperatures (T_g), ranging from 62 to 132 °C, depend strongly on the polymer structure. The longer flexible chain segments lead to lower T_g values. Therefore, the T_g can be adjusted by tuning the polymer structure to accommodate material application requirements. The temperature at which the polymer started to lose weight was recorded as the thermal decomposition temperature (T_d). The main-chain polymers synthesized exhibit good thermostability.

One of the advantages of the random main-chain polymers is that they can be easily synthesized by standard condensation techniques. The vast array of available monomers permit synthesis of many main-chain NLO polymers. This will not only increase the size of the main-chain NLO polymer family but also permit study of the relationship between structure and properties. By careful molecular design, the structure of the polymers can be tuned and materials with desired properties can be obtained. For example, by introducing cross-linking groups from comonomers, cross-linkable main-chain, second-order NLO polymers can be synthesized.

Among the main-chain NLO polymers synthesized, polymer 1 and polymer 4 are cross-linkable. Polymer 4

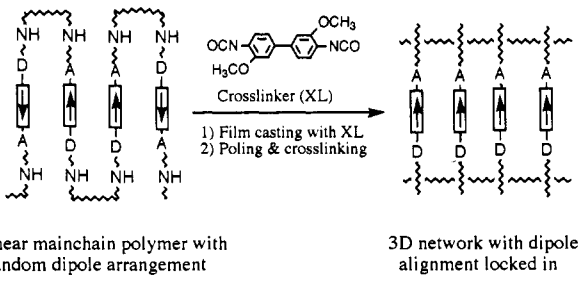

Figure 3. Simplified diagram of the formation of the 3D polymer network with dipole alignment locked in, through electric poling and thermal curing.

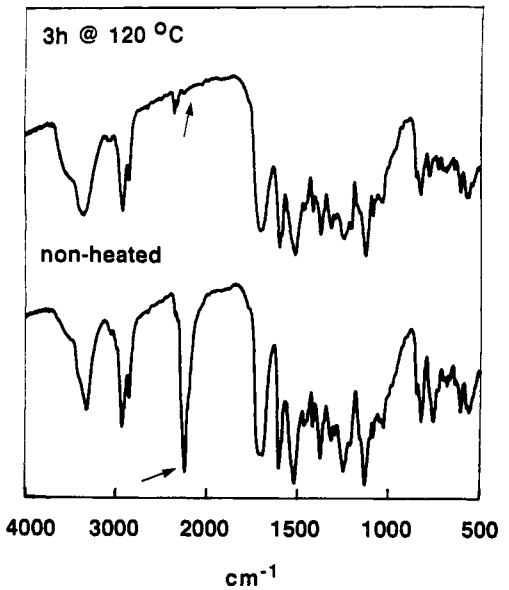

Figure 4. FTIR spectra of polymer 1 before and after curing.

can be cross-linked through the well-known solid-state photoreaction of the cinnamoyl groups.[19,24] The –NH– groups in polymer 1 are active and can react with the isocyanate groups in the cross-linker (XL), 4,4′-diisocyanato-3,3′-dimethoxydiphenyl, to form cross-linked 3D polymer networks. This cross-linking reaction is known as an allophanate reaction. In our experiment, a thin film of polymer 1 containing XL was poled and cured simultaneously to align the chromophore dipoles and lock in the dipole alignment, as illustrated in Figure 3. The cross-linking reaction was monitored by FTIR. Figure 4 gives the FTIR spectra of the polymer 1 samples before and after thermal curing. The characteristic FTIR band (2248 cm^{-1}) of the isocyanate group in XL decreases with progress of curing and completely vanishes after 2 h of curing at 125 °C. The cross-linked films peeled off the glass slides are not soluble in organic solvents, which also confirms the cross-linking of the film.

NLO Properties. Because of the similarity of the chemical properties of the hydroxy groups at the two ends of the monomers (monomers 1 and 2), the chromophore dipoles are expected to be randomly arranged along the backbone of the main-chain polymers (i.e., the dipoles can be head-to-tail, tail-to-tail, or head-to-head). As can be seen from Figure 1c, the dipole moments appear to cancel each other out when a random chain is viewed in extended configuration. Therefore, the poling efficiency of the random main-chain polymers was regarded as a problem. However, for amorphous polymers with appropriate flexible chain segments, the polymer chains prefer the random-coil configurations (Figure 1d). When the

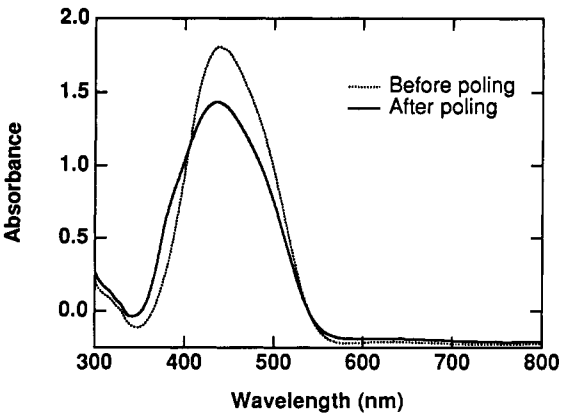

Figure 5. Absorption spectra of polymer 1 before and after electric poling.

Table IV. Linear and Nonlinear Optical Properties of the Polymers

polymer	λ_{max} unpoled	λ_{max} poled	index n_{1064}	index n_{532}	Φ $(1 - A_p/A_0)$	$\langle\cos^3\theta\rangle$	d_{33} (pm/V)	$\chi^{(2)}$ (10^{-7} esu)
1	439	437	1.619	1.729	0.20	0.35	60	2.8
2	436	437	1.652	1.854	0.16	0.31	125	6.0
3	436	436	1.730	1.824	0.14	0.29	125	6.0
4	443	446	1.684	1.899	0.38	0.48	150	7.2
5	436	437	1.571	1.717	0.17	0.32	100	4.8

polymer films are heated near T_g and poled by an electric field the chromophore dipoles will align up with the field through bond rotations of the flexible chain segments to realize noncentrosymmetric order, as illustrated in Figure 1d. Indeed, as shown in Figure 5 and Table IV the main-chain polymers can be efficiently poled by an electric field, yielding large second-order optical nonlinearities.

Figure 5 gives one example of the absorption spectra of the main-chain polymers. The films show no absorption peaks from 800 to 2500 nm. It is noted that an absorbance change occurs after the film is poled. The decrease in absorbance is an indicator of the dipole alignment, and the order parameter can be calculated by the equation, $\Phi = 1 - A_p/A_0$, where A_p is the peak absorbance of the poled film and A_0 is that of the unpoled film. The alignment factor $\langle\cos^3\theta\rangle$, typically 0.3–0.4, can then be calculated from Φ by using the literature method.[3,30] The alignment factor can also be calculated from second-order nonlinear susceptibilty using the oriented-gas model equation, $\chi^{(2)} = Nf_{(2\omega)}f^2_{(\omega)}\beta\langle\cos^3\theta\rangle$, where N is the number density of NLO moiety in a polymer, $f_{(2\omega)}$ and $f_{(2\omega)}$ are the local field factors and β is the first hyperpolarizability. Therefore, the poling efficiency can be approximately determined from the absorption spectra or $\chi^{(2)}$ of the polymer films.

Table IV lists some linear and nonlinear optical properties of the polymers. The absorption peaks are virtually at the same wavelength ($\lambda_{max} \approx 440$ nm), indicating no significant contribution or perturbation to the electronic structures or charge transfer properties of the NLO units from the comonomers. The peak shifts after poling are also negligible, which means the chemical structures of the chromophores are not damaged by heating and poling. Table IV also shows that the main-chain NLO polymers (polymers 1–4) can be efficiently poled, yielding large nonlinearities that are comparable to that of the side-chain polymer (polymer 5) containing the same chromophore. It should be pointed out that the second-order

(30) Page, R. H.; Jurich, M. C.; Reck, B.; Sen, A.; Tweig, R. J.; Swalen, J. D.; Bjorklund, G. C.; Wilson, C. G. *J. Opt. Soc. Am.* **1990**, *B7*, 1239.

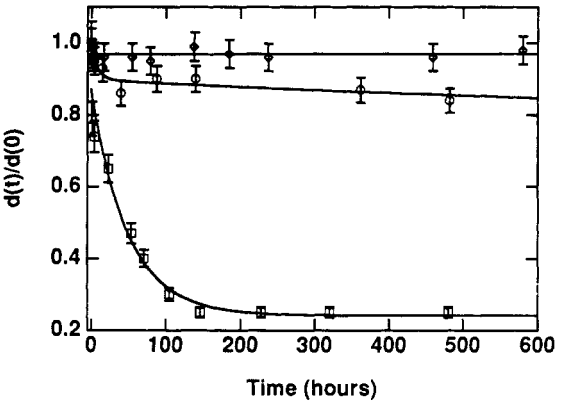

Figure 6. Plot of normalized SHG d coefficients as a function of time at room temperature after the poling electric field was turned off. Square, polymer 1; diamond, polymer 2; circle, polymer 4.

susceptibilities listed in the table are resonance enhanced because of the absorption tail at the second harmonic wavelength (532 nm). Main-chain polymers can be used to optimize the chromophore number density (N), which is determined by the weight fraction of the NLO chromophore in a polymer and the density of the film. In addition to the high weight fraction of the loaded chromophore, as demonstrated in Table III, main-chain polymers can form high-density films because of the tighter packing of individual polymer chains, as suggested by the refractive indexes.

The normalized SHG d coefficients of the polymers, as a function of time after the poling electric field is turned off, are plotted in Figure 6. Polymer 1, containing very long flexible segments between the rigid NLO chromophores, shows a faster decay of nonlinearity than polymer 2 and polymer 4, with shorter flexible segments. This can be interpreted in terms of their chain structures; longer flexible segments favor free segmental motions, as evidenced by the lower T_g. The segmental motion leads to the relaxation of the ordered structure to the thermodynamically more stable random structure. Clearly, stabilization of the poling-induced order and hence the second-order optical nonlinearity can be realized by tuning the polymer structure, such as increasing T_g.

Figure 7 depicts the comparison of the temporal stability between the cross-linked and un-cross-linked films of polymer 1. As is expected, the SHG d coefficient of the cross-linked film has not shown, within experimental

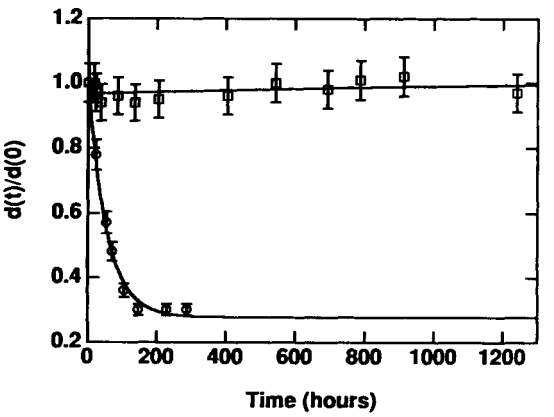

Figure 7. Comparison of temporal NLO stability between the cross-linked (square) and un-cross-linked (circle) polymer 1 films.

error, any significant change for thousands of hours, while that of the un-cross-linked film decays to 25% of the initial value very rapidly. Again, this can be explained by the restriction of the segmental motions after cross-linking. This result demonstrates that the temporal NLO stability can be greatly enhanced by cross-linking the polymer backbone.

Conclusion

We have synthesized several random main-chain, second-order NLO polymers by common condensation polymerization techniques. These polymers can be efficiently poled by an electric field using a corona setup and exhibit large resonance-enhanced optical nonlinearities ($\chi^{(2)} \approx 100$–300 pm/V), which are comparable to the values observed for the side-chain polymers containing the same chromophore. The NLO stability is determined by the polymer chain structure and can be greatly enhanced by crosslinking the polymer mainchains. The flexibility of the design and synthesis of random main-chain NLO polymers allows modification of the polymer structure to further improve the NLO properties such as optical nonlinearity and temporal NLO stability at elevated temperatures.

Acknowledgment. This research is supported by the Air Force Office of Scientific Research (AFOSR) under contracts F49620-91-0270 and F49620-91-0054, by National Science Foundation Grant DMR-91-07806 and by the National Center for Integrated Photonic Technology.